Entropy production for complex Langevin equations

Simone Borlenghi,[1] Stefano Iubini,[2,3] Stefano Lepri,[4,3] and Jonas Fransson[1]
[1]*Department of Physics and Astronomy, Uppsala University, Box 516, SE-75120 Uppsala, Sweden*
[2]*Dipartimento di Fisica e Astronomia, Università di Firenze, via G. Sansone 1 I-50019, Sesto Fiorentino, Italy*
[3]*Istituto Nazionale di Fisica Nucleare, Sezione di Firenze, via G. Sansone 1 I-50019, Sesto Fiorentino, Italy*
[4]*Istituto dei Sistemi Complessi, Consiglio Nazionale delle Ricerche, Via Madonna del Piano 10 I-50019 Sesto Fiorentino, Italy*
(Received 29 March 2017; published 27 July 2017)

We study irreversible processes for nonlinear oscillators networks described by complex-valued Langevin equations that account for coupling to different thermochemical baths. Dissipation is introduced via non-Hermitian terms in the Hamiltonian of the model. We apply the stochastic thermodynamics formalism to compute explicit expressions for the entropy production rates. We discuss in particular the nonequilibrium steady states of the network characterized by a constant production rate of entropy and flows of energy and particle currents. For two specific examples, a one-dimensional chain and a dimer, numerical calculations are presented. The role of asymmetric coupling among the oscillators on the entropy production is illustrated.

DOI: 10.1103/PhysRevE.96.012150

I. INTRODUCTION

Simple oscillator models allow one to tackle fundamental problems of nonequilibrium statistical mechanics [1–4] and to study energy transport in systems that are ubiquitous in physics, chemistry, biology, and nanosciences [5,6]. Examples include, but are not limited to, the dynamics of spin systems [7,8], Bose-Einstein condensates, lasers, mechanical oscillators [9], and photosynthetic reactions [10].

A central issue is to identify the conditions under which a network of oscillators reaches thermal equilibrium or is driven in a nonequilibrium steady state characterized by the propagation of coupled currents. One basic observable characterizing the state is the entropy production, whose calculation in terms of the microscopic variables is the object of the present paper. In particular, we address this issue using the language of stochastic thermodynamics (ST) [11–17]. Within the ST framework, the out-of-equilibrium dynamics is described combining the Langevin and associated Fokker-Planck (FP) equations or a (quantum or classical) master equation [16–21]. Those allow one to define the evolution of probability over the phase space and to derive consistent expressions for thermodynamic forces and flows and for entropy production for states arbitrarily far from equilibrium.

Another issue that can be considered is the presence of asymmetric couplings in the system Hamiltonian. Physical systems that can be described by asymmetrically coupled oscillators include magnetic materials with asymmetric exchange coupling [22], synthetic lattice gauge fields [23], transport in topological insulators [24], and parametrically driven oscillators [25]. Here we discuss how, in a network of coupled oscillators, detailed balance can be broken either by the presence of thermal baths at different temperatures and chemical potential or by an *anti-Hermitian coupling* among the oscillators. The use of anti-Hermitian Hamiltonians to describe phenomenologically irreversibility both in classical and quantum systems has been widely investigated [26–28]. Here we move a step forward by *quantifying* irreversibility in those systems using the ST language.

Although our formulation is completely general, we shall mostly refer to the dynamics of coupled nonlinear oscillators in the form of the discrete nonlinear Schrödinger equation (DNLS) [29–31] whose off-equilibrium properties have received a certain attention recently [8,32–35]. The spin-Josephson effect [36], the connection between gauge invariance and thermal transport [37] and heat or spin rectification [38–40] are a few of the effects within the DNLS field that can be captured by the ST formalism. One appealing feature of this class of models is the presence of two conserved quantities, namely energy and norm [32,33,41], that give rise to coupled transport effects between the associated currents [32]. This constitutes a further element of novelty that has not yet been considered in the existing literature.

The remainder of the paper is organized as follows. In Sec. I we describe the dynamics of a network of complex Langevin equations, and we introduce the associated Fokker-Planck (FP) equation. In Sec. II we derive the entropy flow and entropy production for this system, and in Sec. III we identify the adiabatic and nonadiabatic components of entropy production. In Sec. IV we show the link between heat and entropy flows and report simulations for the specific case of a DNLS chain with boundary thermostats. In Sec. V we discuss example of the dimer, the simplest realisation of the DNLS consisting of only two coupled oscillators. We present some numerical simulations that elucidate its off-equilibrium dynamics. Finally, in Sec. V we conclude the work and summarize the main results.

II. STOCHASTIC NETWORK MODEL

Let us consider a network, where the dynamics of each of the $m = 1, \ldots, M$ nodes is described by the following Langevin equations [see the sketch in Fig. 1(a)]:

$$\dot{\psi}_m = F_m + \xi_m. \tag{1}$$

Here the dot indicates time derivative and $\psi_m = \sqrt{p_m(t)}e^{i\phi_m(t)}$ is a complex oscillator amplitude. The force F_m is an arbitrary function of the ψs and their complex conjugate. We assume that both the coupling between the ψs and the local forcing and damping are contained in the definition of F. The white noises ξ_m, which model the stochastic baths, are complex Gaussian

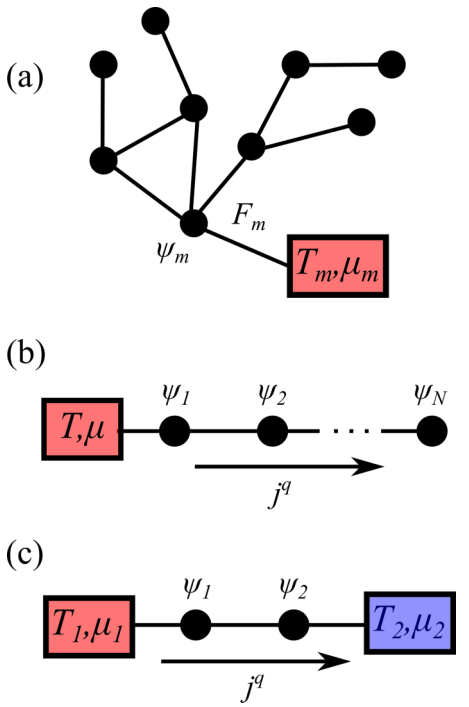

FIG. 1. (a) Network of nonlinear oscillators, where ψ_m is the local oscillator amplitude and F_m the force that specifies the geometry of the system. Each site can be coupled to a thermal bath with temperature T_m and chemical potential μ_m. (b) DNLS chain with the first site connected to a bath with temperature T and chemical potential μ. (c) Schrödinger dimer, consisting of two coupled oscillators connected to two thermal baths with different temperature T_m and chemical potential μ_m, $m = 1,2$.

random processes with zero average and correlation

$$\langle \xi_m(t)\xi_n^*(t')\rangle = D_m\delta_{mn}\delta(t-t'). \tag{2}$$

Here $D_m = \alpha_m T_m$ is the diffusion constant, with α_m the damping rate and T_m the temperature of bath m. Equation (1) is a general model that describes a multitude of systems encountered in physics, chemistry, and biology.

Throughout the paper we adopt the following conventions: We set the Boltzmann constant k_B equal 1. Vectors and matrices are written in plain text, while their component are denoted by the m and n subscripts.

We define the Wirtinger derivatives as

$$\partial_m \equiv \frac{\partial}{\partial\psi_m} = \frac{1}{2}\left(\frac{\partial}{\partial x_m} - i\frac{\partial}{\partial y_m}\right), \tag{3}$$

with $\psi_m = x_m + iy_m$ and $\partial_m^* = \frac{\partial}{\partial\psi_m^*}$ its complex conjugated. The variables $(\psi_m, i\psi_m^*)$ are canonically conjugate. The total forces $F_m = F_m^I + F_m^R$ are the sum of dissipative (or irreversible, I) and conservative (or reversible, R) components. Those are given by the derivatives $F_m^{I/R} = i\partial_m^*\mathcal{H}^{I/R}$ of anti-Hermitian and Hermitian Hamiltonians $\mathcal{H}^{I/R}$, respectively. The latter have opposite parity under the time-reversal transformation and the total Hamiltonian $\mathcal{H}$ is defined as $\mathcal{H} = \mathcal{H}^I + \mathcal{H}^R$.

The Fokker-Planck (FP) equation associated to Eq. (1) reads [42,43]

$$\dot{P} = \sum_m [-\partial_m(F_m P) - \partial_m^*(F_m^* P) + 2D_m\partial_m\partial_m^* P]. \tag{4}$$

Equation (4) gives the evolution of the probability P to find the system in the configuration $(\psi_1,\ldots,\psi_M,\psi_1^*,\ldots,\psi_M^*)$ at time t. Following Refs. [44,45], we define the irreversible and reversible probability currents

$$\mathcal{J}_m^I = F_m^I P - D_m\partial_m^* P, \tag{5}$$

$$\mathcal{J}_m^R = F_m^R P, \tag{6}$$

with $\mathcal{J}_m = \mathcal{J}_m^I + \mathcal{J}_m^R$ and $\mathcal{J}_m^*$ its complex conjugated. In terms of those currents the FP equation, Eq. (4), assumes the form of a continuity equation:

$$\dot{P} = \sum_m(-\partial_m\mathcal{J}_m - \partial_m^*\mathcal{J}_m^*). \tag{7}$$

The steady state corresponds to $\dot{P} = 0$, while thermal equilibrium corresponds to $\mathcal{J}_m = \mathcal{J}_m^* = 0$.

The average of an arbitrary function f of the observables is expressed by means of P as $\langle f\rangle = \int f P dx$, where $dx = (\frac{i}{2})^N\prod_{m=1}^N d\psi_m\wedge d\psi_m^*$ is the phase-space volume element. Note that this average is equivalent to ensemble average of Eq. (1) over different realizations of the stochastic processes. As usual [16,18], we consider the case where the probability currents and the thermodynamical forces vanish at infinity, so that the cross terms in the integration by part can be discarded.

III. ENTROPY FLOW AND ENTROPY PRODUCTION

The entropy flow Φ and entropy production Π are obtained starting from the definition of phase-space entropy

$$S = -\langle\log P\rangle \equiv -\int P\log P dx \tag{8}$$

and computing its time derivative by means of Eq. (4):

$$\dot{S} = \int\sum_m(\partial_m\mathcal{J}_m + \partial_m^*\mathcal{J}_m^*)\ln P dx. \tag{9}$$

On integrating by parts, using Eqs. (5)–(7) and assuming that the reversible forces have zero divergence [18,19], Eq. (9) becomes

$$\dot{S} = -2\mathrm{Re}\int\sum_m\mathcal{J}_m^I\frac{\partial_m P}{P}dx. \tag{10}$$

From Eq. (5) one has

$$\frac{\partial_m P}{P} = \partial_m\ln P = \frac{1}{D_m}\left(F_m^{I*} - \mathcal{J}_m^{I*}/P\right) \tag{11}$$

and $\partial_m^*\ln P$ its complex conjugate. Substituting this into Eq. (10) gives

$$\dot{S} = -2\mathrm{Re}\int\sum_m\mathcal{J}_m^I\frac{F_m^I}{D_m}dx + \int\sum_m\frac{|\mathcal{J}_m^I|^2}{D_m P}dx. \tag{12}$$

The two terms in Eq. (12) correspond respectively to minus the entropy flow Φ from the system to the environment and

entropy production Π. Note in particular that Φ has the usual form of products between probability fluxes $\mathcal{J}_m$ and thermodynamical forces F_m^*/D_m and that Π is positive definite. In nonequilibrium stationary states, one has $\dot{S} = -\Phi + \Pi = 0$, so that $\Phi = \Pi$. These quantities are both zero only at thermal equilibrium. On using Eq. (5), integrating by parts, and substituting the integrals over P with ensemble average, the total entropy flow becomes

$$\Phi = \sum_m \Phi_m = \sum_m \left[2\frac{\langle |F_m^I|^2 \rangle}{D_m} + 2\mathrm{Re}\langle \partial_m F_m^I \rangle \right], \tag{13}$$

where Φ_m is the entropy flow on site m. Note that Eq. (13) is the generalization of the expression given in Ref. [18] to the case where forces are complex valued.

Before concluding the section, let us briefly discuss the more general case of nonstationary conditions. To this aim, it is useful to separate the entropy production into adiabatic and nonadiabatic components, which correspond respectively to steady and nonsteady states [21]. On indicating with superscript s the steady state probability P^s and fluxes $\mathcal{J}^s$, one writes the steady-state FP equation as

$$\dot{P}^s = \sum_m \left[-\partial_m \mathcal{J}_m^s - \partial_m^* \mathcal{J}_m^{*s} \right] \equiv 0. \tag{14}$$

By using Eqs. (5) and (6), it is convenient to define the following quantity:

$$\Lambda_m \equiv \frac{\mathcal{J}_m}{P} - \frac{\mathcal{J}_m^s}{P^s} = -D_m \partial_m^* \ln \frac{P}{P^s}. \tag{15}$$

Equation (15) defines the discrepancy between a stationary and nonstationary state. By inserting Λ_m into the definition of entropy production Eq. (10) and integrating by parts, one can show that the latter splits into the sum $\Pi = \Pi^a + \Pi^{na}$ of two parts which are respectively the adiabatic and nonadiabatic components:

$$\Pi^a = 2\int \sum_m \frac{P}{D_m} \frac{|\mathcal{J}_m^s|^2}{P_s^2} dx = 2\sum_m \left\langle \frac{|\mathcal{J}_m^s|^2}{D_m P_s^2} \right\rangle, \tag{16}$$

$$\Pi^{na} = 2\int \sum_m \frac{P}{D_m} |\Lambda_m|^2 dx = 2\sum_m \left\langle \frac{|\Lambda_m|^2}{D_m} \right\rangle. \tag{17}$$

The adiabatic component corresponds to nonequilibrium steady state, obtained, for example, connecting the system to baths at different constant temperature. On the other hand, the nonadiabatic component corresponds to nonstationary states, obtained by applying a time-dependent driving to the system.

IV. STEADY-STATE HEAT FLOW

Let us return to the stationary case and consider the relation between the entropy flux Φ derived in the previous section and the heat flow. For clarity, we specialize to the relevant case of DNLS oscillators in contact with boundary reservoirs [33]. In particular, we consider the geometry sketched in Fig. 1(b), where the first site of the chain is in contact with a reservoir on the left at temperature T and chemical potential μ and with the rest of the chain on the right. This setup is described by the following Hamiltonians [8]

$$\mathcal{H}^R = \sum_m h_m, \tag{18}$$

$$\mathcal{H}^I = i\alpha(h_1 - \mu p_1), \tag{19}$$

where h_m is the local energy yielding the conservative forces $F_m^R \delta_{mj} = i\partial_m^* h_j$. Analogously, the irreversible forces are $F_m^I \delta_{m1} = i\partial_m^* \mathcal{H}^I$. Let us now evaluate the variation of the local internal energy $u_1 = \langle h_1 - \mu p_1 \rangle$ on a stationary state.

$$\dot{u}_1 = \frac{d}{dt}\int dx\, P(x)(h_1 - \mu p_1) = \int dx\, P(x)(\dot{h}_1 - \mu \dot{p}_1)$$
$$= \frac{1}{i\alpha}\int dx\, P(x)\dot{\mathcal{H}}^I, \tag{20}$$

where $\alpha \neq 0$ is assumed. On substituting the dissipative forces and using the antihermitianity of $\mathcal{H}^I$, one has

$$\dot{u}_1 = \frac{1}{i\alpha}\left\langle \sum_m \left(\frac{\partial \mathcal{H}^I}{\partial \psi_m^*}\dot{\psi}_m^* + \frac{\partial \mathcal{H}^I}{\partial \psi_m}\dot{\psi}_m \right) \right\rangle$$
$$= \frac{1}{i\alpha}\left\langle \left(-iF_1^I \dot{\psi}_1^* - iF_1^{I*}\dot{\psi}_1 \right) \right\rangle. \tag{21}$$

By inserting the equations of motion, Eq. (1), the above equation becomes

$$\dot{u}_1 = -\frac{1}{\alpha}\left[2\langle |F_1^I|^2 \rangle + 2\mathrm{Re}\langle F_1^I \xi_1(t) \rangle \right]$$
$$- \frac{2}{\alpha}\mathrm{Re}\langle F_1^I F_1^{*R} \rangle, \tag{22}$$

assuming that $\langle F_m^I \xi_j \rangle = \alpha T \langle \partial_m F_m^I \rangle$ as in Refs. [18,19], one gets

$$\dot{u}_1 = -\Phi_1 T - \frac{2}{\alpha}\mathrm{Re}\langle F_1^I F_1^{*R} \rangle = -\Phi_1 T - j_1^q, \tag{23}$$

where j_1^q is the heat flux on site 1. Indeed, for a lattice site m in contact with the reservoir, we have

$$j_m^q - j_{m-1}^q = \frac{2}{\alpha}\mathrm{Re}\langle F_m^I F_m^{*R} \rangle$$
$$= -2\mathrm{Re}\left\langle \frac{\partial h_m}{\partial \psi_m^*} F_m^{*R} \right\rangle + 2\mu \mathrm{Re}\left\langle \frac{\partial p_m}{\partial \psi_m^*} F_m^{*R} \right\rangle. \tag{24}$$

The first term of the right-hand side corresponds to the energy flow difference $j_m^h - j_{m-1}^h$ while the second term is the particle flow difference $j_m^p - j_{m-1}^p$ [8] multiplied by the chemical potential. Therefore, we consistently obtain the relation $j_m^q = j_m^h - \mu j_m^p$ [6]. Finally, since $\dot{u}_1 = 0$ on a stationary state and $j_0^q = 0$, we recover the basic thermodynamical relation $j_1^q = -\Phi_1 T$.

The consistency of Eq. (23) has been tested numerically on a chain of L DNLS oscillators in contact with two boundary heat baths. The system Hamiltonian can be explicitly written as

$$\mathcal{H}^R = \sum_{m=1}^{L} (|\psi_m|^4 + \psi_m^* \psi_{m+1} + \psi_{m+1}^* \psi_m) \tag{25}$$

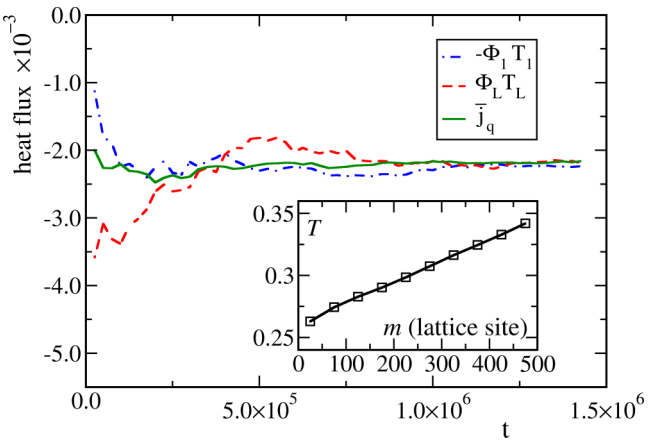

FIG. 2. Heat-flux balance during the relaxation to a nonequilibrium stationary state of a DNLS chain with $L = 500$ lattice sites. The system is in contact with two boundary reservoirs at temperature $T_1 = 0.25$, $T_L = 0.35$ and chemical potential $\mu_1 = \mu_L = -1$, with couplings $\alpha_1 = \alpha_L = 0.05$. Blue (dot-dashed) and red (dashed) curves refer to the boundary heat flux computed from the entropy fluxes Φ_j, with $j = 1, L$. The green (solid) line shows the behavior of the average heat flux $\overline{j_q}$ in the bulk, computed through Eq. (24). The inset shows the temperature profile measured in the stationary regime (see Ref. [32] for computational details). Simulations were performed with a fourth-order Runge-Kutta algorithm with a time step of 0.005 model temporal units.

and the heat baths are implemented as in Eq. (1) with $D_1 = \alpha T_1$ and $D_2 = \alpha T_2$. Assuming fixed boundary conditions ($\psi_0 = \psi_{L+1} = 0$), the dissipative Hamiltonian reads [8,33]

$$\begin{aligned}\mathcal{H}^I = {} & i\alpha(|\psi_1|^4 + \psi_1^*\psi_2 + \psi_2^*\psi_1 - \mu_1 p_1) \\ & + i\alpha(|\psi_L|^4 + \psi_L^*\psi_{L-1} + \psi_{L-1}^*\psi_L - \mu_L p_L).\end{aligned} \tag{26}$$

Figure 2 shows the heat-flux balance between the boundary currents $\Phi_j T_j$ $(j = 1, L)$ and the average bulk flux $\overline{j^q} = 1/L \sum_m j_m^q$ near a nonequilibrium stationary state with different boundary temperatures. When the stationary state is reached, a relation analogous to Eq. (23) holds separately at the rightmost boundary. This regime corresponds to a linear temperature profile along the chain (see the inset) and a flat profile of j_m^q (data not shown).

V. DYNAMICS OF A DIMER

For a better physical insight, and to appreciate the role of coupling on transport, we now discuss the simplest realization of the DNLS consisting of only two coupled oscillators $L = 2$ [see Fig. 1(c) for a schematic]. The system is described by the non-Hermitian Hamiltonian

$$\begin{aligned}\mathcal{H} = {} & (1 + i\alpha)[\omega_1(p_1)p_1 + \omega_2(p_2)p_2 + A_{12}\psi_1\psi_2^* \\ & + A_{21}\psi_1^*\psi_2] + i\alpha\mu_1 p_1 + i\alpha\mu_2 p_2.\end{aligned} \tag{27}$$

The quantities $\omega_m(p_m) = \omega_m^0 + Qp_m$ and $\alpha\omega_m(p_m)$, $m = 1,2$ are, respectively, the nonlinear frequency and damping with Q the nonlinearity coefficient, while μ_m is the chemical potential. For simplicity, we do not write the explicit dependence of the frequencies on the powers. The coupled equations of motion, given by $\dot{\psi}_m = i\partial_m^*\mathcal{H} + \xi_m$, $m = 1,2$ read

$$\dot{\psi}_1 = (i - \alpha)(\omega_1\psi_1 + A_{12}\psi_2) + \alpha\mu_1\psi_1 + \xi_1, \tag{28}$$

$$\dot{\psi}_2 = (i - \alpha)(\omega_2\psi_2 + A_{21}\psi_1) + \alpha\mu_2\psi_2 + \xi_2. \tag{29}$$

From the previous section, one has the following expressions for particle and energy currents:

$$j_{12}^p = 2\mathrm{Im}\langle A_{12}\psi_1^*\psi_2\rangle, \tag{30}$$

$$j_{12}^E = 2\mathrm{Re}\langle A_{12}\psi_1^*\dot{\psi}_2\rangle. \tag{31}$$

When the two reservoirs have different temperatures and/or chemical potentials or an asymmetric coupling, the system reaches a nonequilibrium steady state where the currents are constant. Thermal equilibrium, which corresponds to the case where the currents are zero, is obtained where both baths have the same temperature and chemical potentials and the coupling is symmetric, $A_{12} = A_{21} \equiv A$. Note that if the coupling is symmetric, one has $j_{12}^{p/E} = -j_{21}^{p/E}$. However, for an asymmetric coupling, those currents differ and transport is described by the net currents $j_{\mathrm{net}}^{p/E} = j_{12}^{p/E} - j_{21}^{p/E}$.

As discussed previously, the I and R components of the thermodynamical forces $F_m^{I/R} = i\partial_m^*\mathcal{H}^{I/R}$ are the ones that change (respectively, do not change) sign on the time-reversal operation $\mathcal{H}^{I/R}(t) \to \mathcal{H}^{I/R*}(-t)$. To separate the Hamiltonian in I/R parts, it is convenient to split the coupling between the oscillators as $A = B + C$, respectively, into Hermitian and anti-Hermitian parts. A straightforward calculation gives

$$\begin{aligned}\mathcal{H}^I = {} & -i\alpha(\omega_1 p_1 + \omega_2 p_2 + \mu_1 p_1 + \mu_2 p_2) \\ & - i\alpha(B_{12}\psi_1^*\psi_2 + B_{21}\psi_1\psi_2^*) \\ & + C_{12}\psi_1^*\psi_2 + C_{21}\psi_1\psi_2^*,\end{aligned} \tag{32}$$

$$\begin{aligned}\mathcal{H}^R = {} & \omega_1 p_1 + \omega_2 p_2 + B_{12}\psi_1^*\psi_2 + B_{21}\psi_1\psi_2^* \\ & - i\alpha(C_{12}\psi_1^*\psi_2 + C_{21}\psi_1\psi_2^*),\end{aligned} \tag{33}$$

and the thermodynamical forces read

$$F_1^I = -\alpha(\mu_1\psi_1 + \omega_1\psi_1 + B_{12}\psi_2) - iC_{12}\psi_2, \tag{34}$$

$$F_1^R = -i(\omega_1\psi_1 + B_{12}\psi_2) - \alpha C_{12}\psi_2. \tag{35}$$

Note that one has the same decomposition if the coupling matrix A is real, but in this case B and C are, respectively, its symmetric and antisymmetric components. One can see here that the presence of anti-Hermitian (or antisymmetric) components adds extra terms in both the irreversible and reversible forces.

Following Eq. (13), the entropy production for the dimer finally reads:

$$\Phi = 2\frac{\langle|F_1^I|^2\rangle}{\alpha T_1} + 2\frac{\langle|F_2^I|^2\rangle}{\alpha T_2} + 2\mathrm{Re}\langle\partial_1 F_1^I\rangle + 2\mathrm{Re}\langle\partial_2 F_2^I\rangle, \tag{36}$$

with $\partial_m F_m = -\alpha(\mu_m + \omega_m)$.

We turn now to numerical simulations of Eqs. (28) and (29). In the following, the parameters $\alpha = 0.02$, $\omega_1^0 = \omega_2^0 = 1$ were used. At first, we have calculated the observables for a system

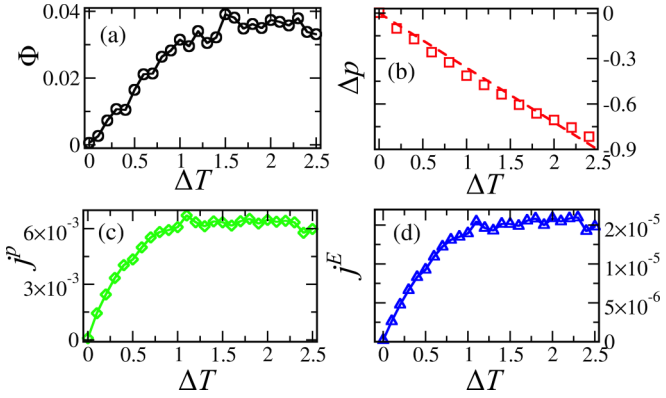

FIG. 3. DNLS dimer: Time-averaged observables as a function of $\Delta T = T_1 - T_2$. Panel (a) shows the entropy flow and panel (b) the power difference $\Delta p = p_1 - p_2$, while panels (c) and (d) display, respectively, particle and energy currents. The solid lines are guides to the eye, while the dashed line in panel (b) is a linear fit. Equations (28) and (29) have been integrated numerically using a fourth-order Runge-Kutta algorithm. The integration has been performed for 4×10^6 steps, with a time step of 10^{-3} model units. The observables where time averaged and then ensemble averaged on 64 different realizations of the thermal field.

with *symmetric* coupling $A_{12} = A_{21} \equiv A = 0.1$, keeping $T_1 = 0.2$ and varying T_2 between 0.2 and 2.7 model units. Figure 3 shows the observables as a function of $\Delta T = T_1 - T_2$. One can see that both the entropy production and the currents increase linearly at low temperature and then saturate. This behavior is similar to what has been observed in several systems previously studied, such as the spin-caloritronics diode and artificial spin chains [8,36,39,40]. It is due to the fact that at increasing temperature, thermal fluctuation hinders synchronization between the oscillators thus reducing the currents.

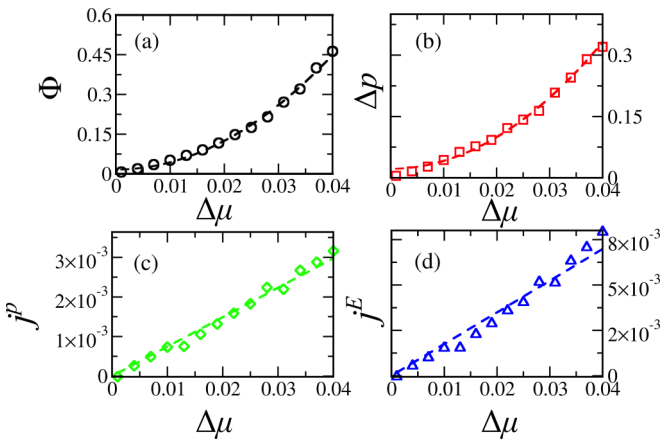

FIG. 4. Time-averaged observables computed as a function of the chemical potential difference $\Delta\mu = \mu_1 - \mu_2$. Panels (a) and (b) show, respectively, the entropy flow and the power difference $\Delta p = p_1 - p_2$, while panels (c) and (d) display, respectively, the particle and energy currents. Dashed lines in panels (a) and (b) are quadratic fits, and dashed lines in panels (c) and (d) are linear fits.

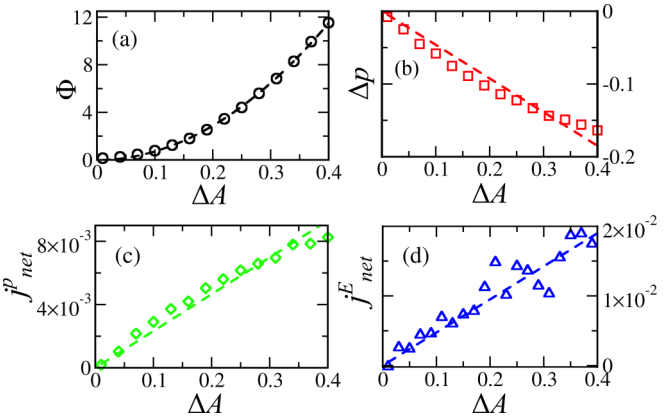

FIG. 5. Time averaged observable at constant temperature, computed as a function of the coupling difference $\Delta A = A_{12} - A_{21}$, keeping $A_{21} = 0.1$ fixed and increasing A_{12}. Panels (a) and (b) show, respectively, the entropy flow and the power difference $\Delta p = p_1 - p_2$, while panels (c) and (d) display, respectively, the particle and energy currents. The dashed line in panel (a) is a quadratic fit, and the dashed lines in panels (b), (c), and (d) are linear fits.

The power difference $\Delta p = p_1 - p_2$ decrease linearly as a function of ΔT, since p_1 remains constant and p_2 is proportional to the temperature T_2.

Next, we focus on the effect of chemical potential difference on transport. In Fig. 4 the observables as a function of $\Delta\mu = \mu_1 - \mu_2$ are reported. The simulations were performed keeping $T_1 = T_2 = 0.1$ and $\mu_2 = 0.01$ fixed and varying μ_1 between 0.01 and 0.05. One can observe that both Φ and Δp grow quadratically, while the currents increase linearly as a function of $\Delta\mu$. Note in particular that no saturation is observed in this case.

Finally, let us discuss the case in which the model is brought outside equilibrium by an asymmetric coupling. Figure 5 displays the observables at constant temperature $T = 0.2$ as a function of the asymmetry $\Delta A = A_{12} - A_{21}$ of the coupling. One can see in Fig. 5(a) that the entropy flow increases quadratically with the coupling, while the other observables are linear in ΔA. Note also that the observables, and in particular the entropy production and the energy current, are much larger than in the case of symmetric coupling and temperature difference, showing that the asymmetric coupling is a very efficient means to drive the system out of equilibrium.

VI. CONCLUSIONS

In summary, we considered assembly of coupled nonlinear oscillators coupled to Langevin baths. Within the ST approach we compute explicit expressions for the entropy production rate and demonstrated their concrete use for specific model cases: the DNLS chain and dimer. In the case of the chain, we showed how the approach to the steady state can be studied by monitoring Φ. For the dimer, we emphasized the role of asymmetry in the coupling as a means to effectively drive the system out of equilibrium. The asymmetry reflects the presence of anti-Hermitian components in the Hamiltonian.

The role of non-Hermitian Hamiltonians in classical and quantum oscillators has been long investigated [26]. Recently,

the differences between the Lindblad and non-Hermitian formulation of open quantum systems have been clarified [46]. The present work can serve to elucidate how anti-Hermitian components contribute to drive out of equilibrium this kind of system. Generalizing these results to the case of multiplicative noise should allow us to treat genuinely quantum systems and provide a connection with the formalism of quantum state diffusion equations [47].

The importance of the dimer is that it is the simplest object that can be investigated, and yet it exhibits a rich dynamics due to the fact that it has two conserved quantities with associated currents. In magnetic system and in particular in spin valve structures, the dipolar interaction between layers introduces naturally an asymmetric coupling [48], and further investigation is needed to understand coupled transport in those systems. Most of the times these setups can be described by simple dimer models as the one treated in this paper [7].

Generally speaking, the off-equilibrium observables are of importance to quantify irreversibility in a multitude of physical systems. Possible applications include the description of transport in mechanical oscillators [25], synthetic gauge fields [23], and topological insulators [24]. Similar expression for entropy productions have also been obtained in the context of granular media [49].

We remark that the role of asymmetric coupling in the dynamics of oscillator network has attracted a certain attention in recent years, especially in connection with synchronisation phenomena and the dynamics of neural network [50–54]. Our work moves a step forward by addressing the off-equilibrium thermodynamics of those type of systems using a very general approach.

We mention also that a possible mechanism to create an asymmetric or complex coupling consists in forcing parametrically the coupled oscillators in such a way that the forcing has a fixed phase.

ACKNOWLEDGMENTS

We thank V. Tosatti and M. Polettini for illuminating discussions. This research was supported by the Stiftelsen Olle Engkvist Byggmästare.

[1] F. Bonetto, J. L. Lebowitz, and L. Rey-Bellet, in *Mathematical Physics 2000*, edited by A. Fokas, A. Grigoryan, T. Kibble, and B. Zegarlinsky (Imperial College, London, 2000), p. 128.
[2] S. Lepri, R. Livi, and A. Politi, Phys. Rep. **377**, 1 (2003).
[3] A. Dhar, Adv. Phys. **57**, 457 (2008).
[4] G. Basile, L. Delfini, S. Lepri, R. Livi, S. Olla, and A. Politi, Eur. Phys J. Spec. Top. **151**, 85 (2007).
[5] A. A. Balandin and D. L. Nika, Mater. Today **15**, 266 (2012).
[6] S. Lepri (ed.), *Thermal Transport in Low Dimensions: From Statistical Physics to Nanoscale Heat Transfer*, Vol. 921 of Lecture Notes in Physics (Springer-Verlag, Berlin, 2016).
[7] A. Slavin and V. Tiberkevich, IEEE Trans. Magn. **45**, 1875 (2009).
[8] S. Borlenghi, S. Iubini, S. Lepri, J. Chico, L. Bergqvist, A. Delin, and J. Fransson, Phys. Rev. E **92**, 012116 (2015).
[9] P. G. Kevrekidis, *The Discrete Nonlinear Schrödinger Equation* (Springer Verlag, Berlin, 2009).
[10] S. Iubini, O. Boada, Y. Omar, and F. Piazza, New J. Phys. **17**, 113030 (2015).
[11] G. E. Crooks, Phys. Rev. E **60**, 2721 (1999).
[12] D. J. Evans and D. J. Searles, Adv. Phys. **51**, 1529 (2002).
[13] U. Seifert, Phys. Rev. Lett. **95**, 040602 (2005).
[14] M. Esposito and S. Mukamel, Phys. Rev. E **73**, 046129 (2006).
[15] S. Deffner and E. Lutz, Phys. Rev. Lett. **107**, 140404 (2011).
[16] M. Esposito, Phys. Rev. E **85**, 041125 (2012).
[17] U. Seifert, Rep. Prog. Phys. **75**, 126001 (2012).
[18] T. Tomé, Braz. J. Phys. **36**, 1285 (2006).
[19] T. Tomé and M. J. de Oliveira, Phys. Rev. E **82**, 021120 (2010).
[20] T. Tomé and M. J. de Oliveira, Phys. Rev. Lett. **108**, 020601 (2012).
[21] C. Van den Broeck and M. Esposito, Phys. Rev. E **82**, 011144 (2010).
[22] S. Cheong and M. Mostovoy, Nat. Mater. **6**, 13 (2007).
[23] A. Celi, P. Massignan, J. Ruseckas, N. Goldman, I. B. Spielman, G. Juzeliūnas, and M. Lewenstein, Phys. Rev. Lett. **112**, 043001 (2014).
[24] A. Rivas and M. A. Martin-Delgado, arXiv:1606.07651.
[25] G. Salerno and I. Carusotto, Europhys. Lett. **106**, 24002 (2014).
[26] H. Dekker, Phys. Rep. **80**, 1 (1981).
[27] S. Rajeev, Ann. Phys. **322**, 1541 (2007).
[28] I. Rotter, J. Phys. A **42**, 153001 (2009).
[29] J. C. Eilbeck, P. S. Lomdahl, and A. C. Scott, Physica D **16**, 318 (1985).
[30] P. G. Kevrekidis, K. O. Rasmussen, and A. R. Bishop, Int. J. Mod. Phys. B **15**, 2833 (2001).
[31] J. C. Eilbeck and M. Johansson, in *Proceedings of the Third Conference: Localization & Energy Transfer in Nonlinear Systems* (World Scientific, Singapore, 2003), p. 44.
[32] S. Iubini, S. Lepri, and A. Politi, Phys. Rev. E **86**, 011108 (2012).
[33] S. Iubini, S. Lepri, R. Livi, and A. Politi, J. Stat. Mech.: Theory Exp. (2013) P08017.
[34] M. Kulkarni, D. A. Huse, and H. Spohn, Phys. Rev. A **92**, 043612 (2015).
[35] C. B. Mendl and H. Spohn, J. Stat. Mech: Theory Exp. (2015) P08028.
[36] S. Borlenghi, S. Iubini, S. Lepri, L. Bergqvist, A. Delin, and J. Fransson, Phys. Rev. E **91**, 040102 (2015).
[37] S. Borlenghi, Phys. Rev. E **93**, 012133 (2016).
[38] J. Ren and J.-X. Zhu, Phys. Rev. B **88**, 094427 (2013).
[39] S. Borlenghi, W. Wang, H. Fangohr, L. Bergqvist, and A. Delin, Phys. Rev. Lett. **112**, 047203 (2014).
[40] S. Borlenghi, S. Lepri, L. Bergqvist, and A. Delin, Phys. Rev. B **89**, 054428 (2014).
[41] K. Ø. Rasmussen, T. Cretegny, P. G. Kevrekidis, and N. Grønbech-Jensen, Phys. Rev. Lett. **84**, 3740 (2000).
[42] H. Z. Haken, Z. Physik **219**, 246 (1969).
[43] T. Xü-Bing and F. Hong-Yi, Commun. Theor. Phys **53**, 1049 (2010).

[44] R. E. Spinney and I. J. Ford, Phys. Rev. E **85**, 051113 (2012).
[45] G. T. Landi, T. Tomé, and M. J. de Oliveira, J. Phys. A **46**, 395001 (2013).
[46] K. G. Zloshchastiev and A. Sergi, J. Mod. Optics **61**, 1298 (2014).
[47] N. Gisin and I. C. Percival, J. Phys. A **25**, 5677 (1992).
[48] V. V. Naletov, G. de Loubens, G. Albuquerque, S. Borlenghi, V. Cros, G. Faini, J. Grollier, H. Hurdequint, N. Locatelli, B. Pigeau, A. N. Slavin, V. S. Tiberkevich, C. Ulysse, T. Valet, and O. Klein, Phys. Rev. B **84**, 224423 (2011).
[49] G. Gradenigo, A. Puglisi, and A. Sarracino, J. Chem. Phys. **137**, 014509 (2012).
[50] H. Yamada, Progr. Theor. Phys. **108**, 13 (2002).
[51] B. Blasius, Phys. Rev. E **72**, 066216 (2005).
[52] I. Belykh, V. Belykh, and M. Hasler, Chaos **16**, 015102 (2006).
[53] M. Zeitler, A. Daffertshofer, and C. C. A. M. Gielen, Phys. Rev. E **79**, 065203 (2009).
[54] C. Cantos, D. K. Hammond, and J. J. P. Veerman, Eur. Phys. J. Spec. Top. **225**, 1199 (2016).